Phase Diagrams of Advanced Magnesium Alloys Containing Al, Ca, Sn, Sr, and Mn

Joachim Gröbner, Andres Janz, Artem Kozlov, Djordje Mirković, and Rainer Schmid-Fetzer

In this paper an overview of the most relevant phase diagrams is given comprising the unconventional alloying elements Sn, Ca, and Sr, in reasonable combinations with Al and Mn in Mg alloys as a basis for advanced applications. The focus is on magnesium-rich partial projections of the liquidus surface of five ternary systems, relevant to technological applications for lightweight materials. All phase diagrams are calculated from a coherent thermodynamic multicomponent database for magnesium alloys. These calculations are validated by key samples in the pertinent subsystems, including extensive ternary assessments and also quaternary work. Isothermal sections of magnesium-rich phase diagrams of alloys with constant aluminum and manganese content at 500ºC and 550ºC are given for the two five-component systems: Mg-Al-Mn-Ca-Sr and Mg-Al-Mn-Ca-Sn.

INTRODUCTION

In traditional alloy development, experimental investigations are performed with many different alloy compositions. The selection criteria for multicomponent alloying elements and their compositions become diffuse in a traditional approach. Computational thermochemistry based on the Calphad approach can provide a clear guideline for such selections and may help to avoid large-scale experiments with less promising alloys. Thus, it is a powerful tool to cut down on cost and time during development of magnesium alloys. A comprehensive overview of the Calphad method is given by H.L. Lukas et al.[1] More details on the ongoing development of a major thermodynamic database for magnesium alloys, currently comprising 20 components (Ag-Al-C-Ca-Ce-Cu-Fe-Gd-Li-Mg-Mn-Nd-Ni-Sc-Si-Sn-Sr-Y-Zn-Zr) and 412 phases are given elsewhere.[2,3] Important aspects of quality assurance in a thermodynamic magnesium alloy database are discussed in Reference 4; there it is emphasized that four different dimensions of quality in a thermodynamic database need to be considered for each binary/ternary dataset: correctness (producing the intended stable phase diagram), reasonability (producing realistic thermodynamic properties), accuracy (producing a satisfactory agreement with all trustworthy experimental data), and safety (producing extrapolations to higher-order systems without artifacts due to precarious treatment of metastable regions).

The combination of light weight, high specific strength, and good castability makes magnesium alloys a promising engineering material for the automotive and aerospace industries.[5–7] Mg-Al-based alloys, especially the AZ and AM series, combine good room-temperature strength and ductility with satisfying salt-spray corrosion resistance and excellent castability. Sufficient creep resistance at elevated temperatures is also required by special automotive applications, such as engine blocks or powertrain components. For these elevated-temperature applications new magnesium alloys were developed on the basis of calcium and strontium additions or rare earth (RE). A.A. Luo[8] discussed the potential of these alloys and demonstrated promising results on the high-temperature strength for magnesium-based alloys with strontium and calcium, but called attention to possible castability problems like sticking and cracking. Additions of RE elements show similar advantages, but should be minimized considering their high costs.

M. Pekguleryuz and E. Baril[9] showed that die-cast Mg-Al-Ca (AX) alloys offer creep resistance, tensile strength, and corrosion resistance comparable to commercially used magnesium alloys with RE additions, like AE42. These properties can be achieved with much lower costs, while the stability of these Al_2Ca precipitates is comparable to the RE precipitates.

Creep resistance, mechanical properties, and microstructure of Mg-Al-Sr (AJ) alloys with less than 7 wt.% aluminum and 3 wt.% strontium were studied by E. Baril et al.[10] They report good creep resistance and excellent castability for such alloys, showing a microstructure consisting of a lamellar phase Al_4Sr at the grain boundaries of

How would you…

…describe the overall significance of this paper?

The development of multicomponent Mg-alloys can be focused on promising areas by using computational thermochemistry. The calculated phase diagrams in this work provide a concise graphical overview for this application.

…describe this work to a materials science and engineering professional with no experience in your technical specialty?

An overview of most relevant phase diagrams for advanced development of magnesium alloys with Sn, Ca, and Sr is presented.

…describe this work to a layperson?

Reducing the weight of future automobiles is a key issue in energy saving and reducing CO_2 emission. A tool is presented here to help the efficient design of the most promising new magnesium alloys for that purpose.

primary magnesium.

In Mg-Al-Sn (AT) alloys the alloying elements improve the castability of magnesium by reducing the melting point, with the advantage that the overall alloy strength is not compromised. It was suggested quite early[11] that the addition of tin improves strength at the expense of ductility in magnesium alloys. Alloys of this series are quite new in application; H. Liu et al.[12] reported recently the tensile properties and creep resistance of as-cast Mg–Sn alloys comparative with that of AE42 alloy at room temperature and at 150ºC and 175ºC.

For magnesium alloys of the most popular AZ series (magnesium-rich Mg-Al-Zn-Mn) the application of thermodynamic calculation for a proper interpretation of liquidus and solidus temperatures was demonstrated earlier.[13] This work will focus on the promising alloy series Mg-Al-Ca (AX), Mg-Al-Sr (AJ), Mg-Ca-Sn (XT), and Mg-Al-Sn (AT) and the combination of these. Additional manganese, present in all industrial magnesium alloys to control the corrosion impact of iron, is also included. A concise selection of calculated isothermal phase diagram sections in the magnesium-rich corner is presented for a better understanding of these more advanced alloy series.

RELEVANT TERNARY SUBSYSTEMS

It is generally accepted in the Calphad community that reliable calculations of multicomponent phase diagrams require the thermodynamic descriptions not only of the binary subsystems but also of the relevant ternary subsystems. The completeness of these descriptions also provides an indication of composition limitations for such calculations.

Within the potential six-component system Mg-Al-Ca-Mn-Sn-Sr a total of ten ternary Mg-X_1-X_2 systems exists. The most important alloying element in such magnesium-based alloys is aluminum. All four Mg-Al-X_1 systems are covered by thermodynamic assessments, as given in Table I, and also Mg-Ca-Sn and Mg-Ca-Sr. The four missing ternaries are Mg-Mn-X_1 (X_1 = Ca, Sn, Sr) and Mg-Sn-Sr. The next level of possibly relevant systems comprises the Al-X_1-X_2 systems, which are remote to

Table I. Ternary and Higher Systems Investigated in Mg-Al-Ca-Mn-Sn-Sr Alloys

System	Number of Key Samples	Number of Invariant Reactions Confirmed	Comment	Reference
Mg-Al-Mn	[a]	2	Mg-rich corner	21
Mg-Al-Ca	4	4	Large ternary solubilities of C14–Mg_2Ca, C15 –Al_2Ca + additional ternary phase C36	23
Mg-Al-Sr	7	7	Large ternary solubilities of $Mg_{38}Sr_9$, $Mg_{17}Sr_2$, Mg_2Sr, $Mg_{23}Sr_6$, Al_4Sr and Al_2Sr + additional ternary phase τ	24
Mg-Al-Sn	9	3	Ternary liquid immiscibility	25
Mg-Ca-Sn	20	6	$Ca_{2-x}Mg_xSn$ phase dominant	27
Mg-Ca-Sr	2	2	Continuous solubility of C14 - $Mg_2(Ca,Sr)$	19
Al-Ca-Sr	3	1	Large ternary solubilities of Al_4Ca, Al_4Sr, Al_2Ca and Al_2Sr	19
Mg-Al-Ca-Sr	2	2	—	19
Mg-Al-Ca-Mn-Sr	2[b]	1	—	19

[a] Experimental literature data; [b]additional magnesium-rich alloys.

Table II. Solid Phases Known To Be in Equilibrium with (Mg) in Mg-Al-Ca-Mn-Sn-Sr Alloys

Phase	Crystal Structure	Remark
γ-$Mg_{17}Al_{12}$	*cI*58 αMn A12 body centered	Dissolves up to 6.8 wt.% Ca and less than 1 wt.% Sr
C14 - $Mg_2(Ca, Sr)$	*hP*12 C14 Laves phase $MgZn_2$	Continuous solubility between Mg_2Ca and Mg_2Sr Dissolves up to 12 wt.% Al
C15 – Al_2Ca	*oF*48 C15 Laves phase $MgCu_2$	Dissolves up to 5 wt.% Mg
C36	*hP*24 C36 Laves phase $MgNi_2$	Stable between 833 and 438°C
$Mg_{17}Sr_2$	*hP*38 Th_2Ni_{17}	Dissolves up to 16 wt.% Al and 2.6 wt.% Ca
Al_4Sr	*tI*10 $BaAl_4$	Dissolves up to 10 wt.% Mg
τ, $Al_{38}Mg_{58}Sr_4$	Not certain	Stable below 477°C
Mg_2Sn	*cF*12 CaF_2	No solubilities observed
CMS $Ca_{2-x}Mg_xSn$ (x=0-1)	*oP*12 Co_2Si	Ca_2Sn dissolves up to 33 at.% Mg
βMn	*cP*20 βMn Cub_A13	Dissolves up to 24 wt.% Al and 0.07 wt.% Mg
αMn	*cI*58 αMn A12 body centered	Dissolves up to 7 wt.% Al and less than 0.001 wt.% Mg
Al_8Mn_5	*hR*26 Al_8Cr_5	No ternary solubilities
$Al_{11}Mn_4$ (HT)	*oP*156 $Al_{11}Mn_4$	No ternary solubilities

Table III. Invariant Four-phase Reactions Involving Liquid and (Mg) in the Six Investigated Ternary Mg-systems*

System	Invariant Reaction	Temperature
Mg-Al-Ca	L = (Mg) + C14 + C36	515°C
	L + C36 = (Mg) + γ-$Mg_{17}Al_{12}$	454°C
Mg-Al-Mn	L + βMn = (Mg) + Al_8Mn_5	637°C
Mg-Al-Sr	L + $Mg_{17}Sr_2$ = (Mg) + Al_4Sr	527°C
	L + Al_4Sr = (Mg) + τ	477°C
	L = (Mg) + γ-$Mg_{17}Al_{12}$ + τ	436°C
Mg-Al-Sn	L = (Mg) + γ-$Mg_{17}Al_{12}$ + Mg_2Sn	431°C
Mg-Ca-Sn	L = (Mg) + $Ca_{2-x}Mg_xSn$ + Mg_2Sn	563°C
	L = (Mg) + $Ca_{2-x}Mg_xSn$ + Mg_2Ca	515°C
Mg-Ca-Sr	L = (Mg) + $Mg_{17}Sr_2$ + C14	510°C

*Results from validated thermodynamic calculations.

the magnesium corner but at least all contain aluminum. There are six of these ternaries and only the Al-Ca-Sr system is assessed. A critical literature review of the other five systems can be found in the MSIT Ternary Evaluation Program. Extensive experimental data are available for Al-Mn-Sr only,[14] showing an extended liquid immiscibility but no ternary compounds. In the Al-Sn-Sr and Al-Ca-Mn systems, only the existence of compounds $Sr_3Al_2Sn_2$,[15] $CaMn_4Al_8$, and $Ca(Mn_xAl_{1-x})_2$ with x = 0.08 to 0.16[16] is known, but not their phase stabilities or melting points. Almost nothing is known about the Al-Ca-Sn[17] and Al-Mn-Sn[18] systems. It may be concluded that the missing ternary thermodynamic descriptions of these five Al-X_1-X_2 systems is not critical for a calculation of pertinent magnesium-rich phase diagrams. This may also be assumed for the last four ternary subsystems of the Ca-Mn-Sn-Sr quaternary, comprising minority components only.

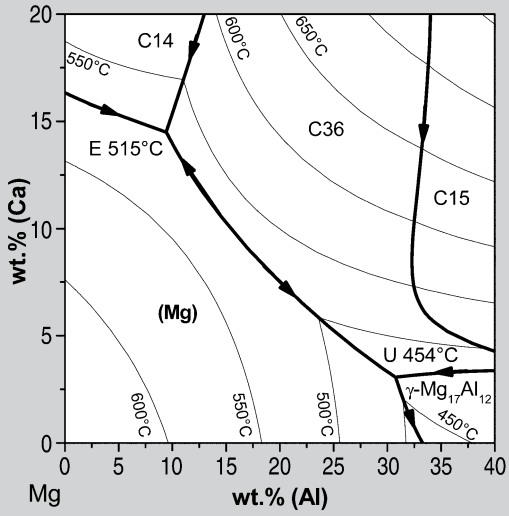

Figure 1. The Mg-Al-Ca liquidus projection for magnesium-rich alloys.

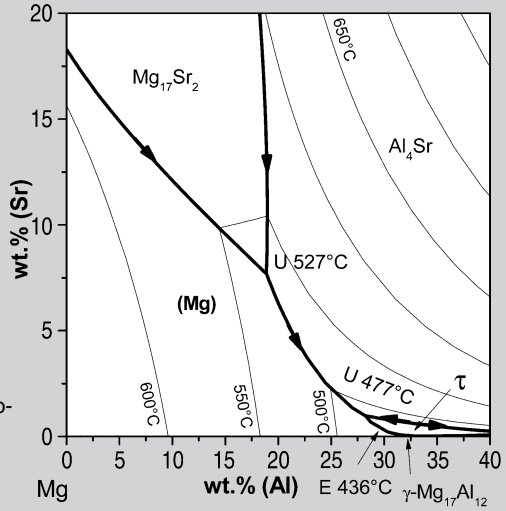

Figure 2. The Mg-Al-Sr liquidus projection for magnesium-rich alloys.

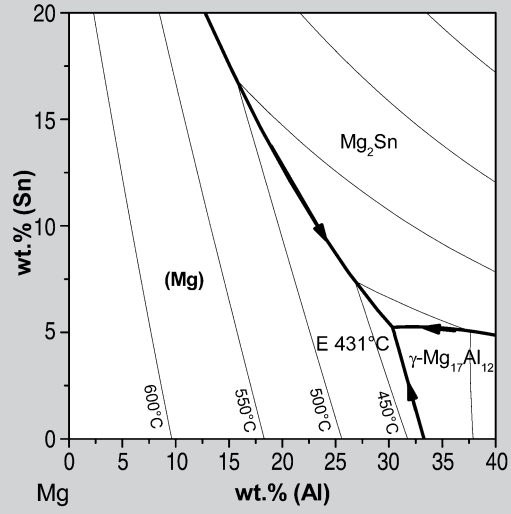

Figure 3. The Mg-Al-Sn liquidus projection for magnesium-rich alloys.

Coherent thermodynamic descriptions have been developed by the authors for the systems listed in Table I. Also highlighted from that work is the use of specific key samples to verify the most relevant invariant reactions identified by thermodynamic calculations. This method was recently extended to multicomponent systems and applied to the quaternary Mg-Al-Ca-Sr and quinary Mg-Al-Ca-Mn-Sr systems,[19] also given in Table I.

A huge number of intermetallic phases exist in the Mg-Al-Ca-Mn-Sn-Sr system. However, the subset of solid phases known to be in equilibrium with (Mg) is rather concise; it is compiled in Table II, together with structural data and important solubility ranges.

Ternary invariant liquidus reactions involving (Mg) are given in Table III. In most cases these are simple eutectic reactions. More complex cases will be discussed below. All phase diagrams in this study are calculated using the software package *Pandat*[20] and the thermodynamic magnesium-alloy database[3,4] into which the current thermodynamic descriptions are incorporated.

Before approaching the quinary phase diagrams it is useful to briefly discuss the most important ternary phase equilibria. These are given concisely as projections of the magnesium-rich liquidus surfaces in Figures 1 to 5. This has already been presented for the Mg-Al-Mn alloys[21] and is not duplicated here. The subsequent revision of the Mg-Al-Mn thermodynamic description[22] does not change the magnesium corner. A convenient Cartesian plot is chosen for all the magnesium-rich partial phase diagrams.

Mg-Al-Ca Alloys

The liquidus surface of the Mg-Al-Ca system is dominated in the magnesium-rich part by the large field of primary crystallized (Mg) in Figure 1. With higher calcium content two different Laves phases, C14 or C36, form

primary, depending on the aluminum content. With less than 3 wt.% calcium and more than 30 wt.% aluminum the γ-$Mg_{17}Al_{12}$ phase is formed, which dissolves up to 6.8 wt.% calcium in the solid state. This solid solution is relevant for corrosion properties since it changes the local properties of γ-$Mg_{17}Al_{12}$ precipitates. The third Laves C15 is in equilibrium with (Mg) only in the solid state below 438ºC, when the C36 phase is no longer stable. This solidification behavior of Mg-Al-Ca alloys is well established with detailed experimental investigations summarized in the most recent thermodynamic assessment.[23] The lowest invariant liquidus reaction with (Mg) is of transition-type, U at 454ºC, from which it descends into the binary eutectic L = (Mg) + γ-$Mg_{17}Al_{12}$ at 439ºC. A maximum is observed at 526ºC, L ↔ (Mg) + C36, beyond which the ternary eutectic L = (Mg) + C14 + C36 occurs at 515ºC.

Mg-Al-Sr Alloys

This system is determined by large ternary solid solubilities in most of the binary phases.[24] Jointly with (Mg) four other phases may form primary crystals from the melt: $Mg_{17}Sr_2$ (containing up to 16 wt.% aluminum), Al_4Sr, γ-$Mg_{17}Al_{12}$ and the ternary phase τ, $Al_{38}Mg_{58}Sr_4$ (see Figure 2). In contrast to the high calcium solubility in γ-$Mg_{17}Al_{12}$, only less than 1 wt.% strontium can be dissolved in this phase. At higher strontium content a separate ternary phase τ, $Al_{38}Mg_{58}Sr_4$, is formed in slowly solidified Mg-Al-Sr alloys.[24]

Mg-Al-Sn Alloys

For the Mg-Al-Sn system the magnesium-rich liquidus projection (Figure 3) is quite simple. The Calphad assessment of Reference 25 reveals that only two phases were formed besides (Mg): Mg_2Sn and, below 5.3 wt.% tin, γ-$Mg_{17}Al_{12}$. At much lower magnesium content the liquidus surface is complex because a large ternary liquid immiscibility produces intricate phase equilibria. This is not relevant for the partial phase diagram in Figure 3 but may deserve attention if a residual liquid phase in a multicomponent Scheil solidification calculation moves into a magnesium-poor region, well below 50 wt.% magnesium.

Mg-Ca-Sn Alloys

The projection of the magnesium-rich liquidus of the Mg-Ca-Sn system in Figure 4 is dominated by the $Ca_{2-x}Mg_xSn$ phase, denoted as CMS, formed by an extended magnesium-solubility of the Ca_2Sn phase. In equilibrium with (Mg) this phase has a composition of x≈1, or CaMgSn, which is the maximum magnesium solubility in Ca_2Sn. Since the stability of this phase is essential for the reliability of the ternary calculation, the thermodynamic modeling of the Ca-Sn binary system has to be done carefully. A thermodynamic assessment of this binary based on finite temperature quantities from first-principle calculations for the solid phases and key experiments was performed previously.[26] The Calphad assessment for the ternary system is given by Reference 27, which was also validated with magnesium-rich cast alloys.[28] The two ternary eutectics given in Table III are connected by a eutectic

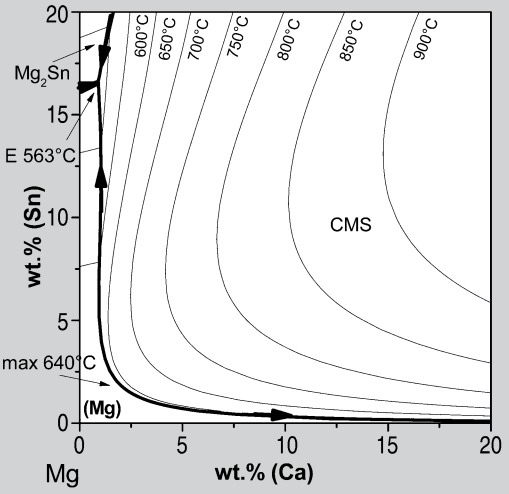

Figure 4. The Mg-Ca-Sn liquidus projection for magnesium-rich alloys; CMS is a shorthand for the $Ca_{2-x}Mg_xSn$ intermetallic phase.

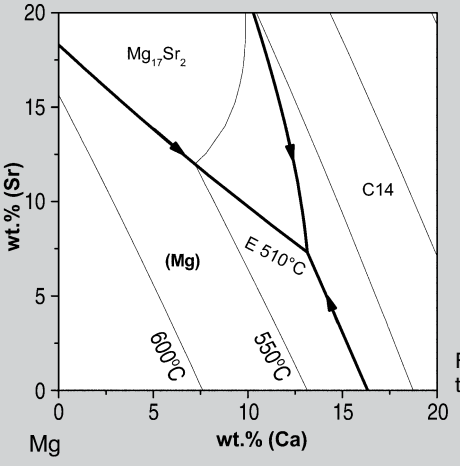

Figure 5. The Mg-Ca-Sr liquidus projection for magnesium-rich alloys.

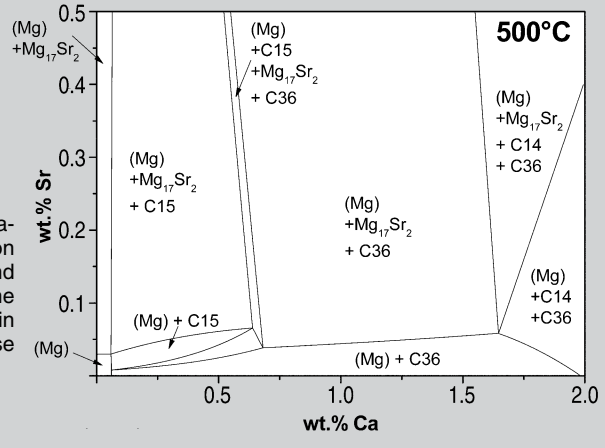

Figure 6. An Mg-Al-Mn-Ca-Sr phase diagram section at 500ºC with 3 wt.% Al and 0.22 wt.% Mn constant. The phase Al_8Mn_5 is stable in small amounts in all phase fields.

trough with a maximum L ↔ $Ca_{2-x}Mg_{x}$-Sn + (Mg) at 640ºC quite near to the magnesium corner shown in Figure 4.

Mg-Ca-Sr Alloys

The magnesium-rich corner of the Mg-Ca-Sr liquidus shows a simple eutectic at 510ºC in Figure 5.[19] However, at that point $Mg_{17}Sr_2$ contains 2.6 wt.% calcium and the C14 phase, which forms a continuous solution range between Mg_2Ca and Mg_2Sr, contains 11.8 wt.% strontium. This solution range completely separates the Mg-Mg_2Ca-Mg_2Sr phase diagram from the magnesium-poor part.

MULTICOMPONENT Mg(-Al-Mn)-Ca-Sr ALLOYS

The validation of multicomponent calculations was methodically elaborated recently.[19] This method was then applied to the Mg-Al-Ca-Sr and Mg-Al-Mn-Ca-Sr systems, and the most relevant invariant reactions could be verified by specifically designed key samples.[19] For the quaternary system two real five-phase invariant reactions could be confirmed. In the five-component system one invariant reaction was verified using a specific key sample and additional validation was based on magnesium-rich commercial alloys.

In the following the constitution of such complex multicomponent magnesium alloys will be highlighted by comparing a selection of calculated phase diagrams for two five-component systems: Mg-Al-Mn-Ca-Sr and Mg-Al-Mn-Ca-Sn. For simplicity, magnesium-rich phase diagram sections at constant aluminum and manganese content are shown at 500ºC and 550ºC. Relevant compositions with 3 wt.% or 9 wt.% aluminum and 0.22 wt.% manganese were chosen. An interesting general result is the presence of the phase Al_8Mn_5 in all these sections. Under these conditions Al_8Mn_5 has formed as a primary phase from the liquid and is present in very small amounts. In order to enhance readability it is not labeled in the diagrams even though it is stable in all phase fields, as noted only in the figure captions.

Figure 6 shows an isothermal section of the Mg-Al-Mn-Ca-Sr system at 500ºC with constant 3 wt.% aluminum and 0.22 wt.% manganese. It shows a small range of homogeneous solid solution (Mg) matrix phase (plus the omnipresent Al_8Mn_5) to be stable at very low calcium and strontium contents. With more strontium the phase $Mg_{17}Sr_2$ is formed, and with more calcium the Laves phases C15 or C36 appear. The third Laves phase, C14, can be observed additionally at calcium content higher than 1.6 wt.%. A dramatic change occurs at only 50ºC higher temperature: all these Laves phases are already molten in this alloy range. A magnified calcium range is shown in Figure 7. Only the $Mg_{17}Sr_2$ phase is still stable.

A significant change occurs in all phase diagram sections with the higher aluminum content of 9 wt.% aluminum: At the corner of the base alloy with 9 wt.% aluminum (and 0.22 wt.% manganese) the completely solid region disappears and alloys become partially liquid. This is best understood by reviewing the binary Mg-Al diagram in Figure 8, showing the base points of the 3 wt.% and 9 wt.% aluminum alloys. In the quinary phase diagram section at 9 wt.% aluminum and 500ºC (Figure 9)

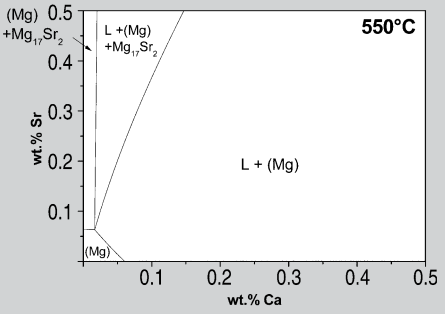

Figure 7. An Mg-Al-Mn-Ca-Sr phase diagram section at 550ºC with 3 wt.% Al and 0.22 wt.% Mn constant. The phase Al_8Mn_5 is stable in small amounts in all phase fields.

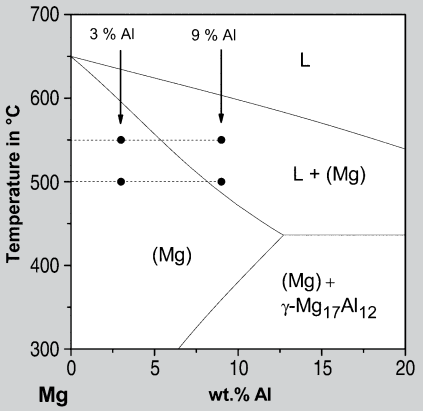

Figure 8. A magnesium-rich part of the binary Mg-Al phase diagram including the compositions of the corner for the five-component phase diagrams in Figures 6, 7, and 9 to 14.

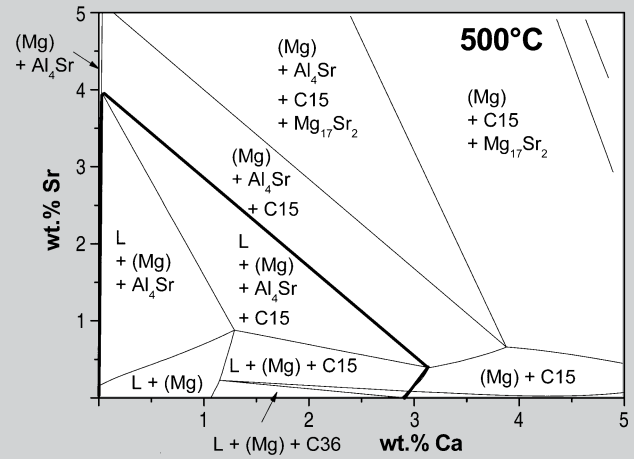

Figure 9. An Mg-Al-Mn-Ca-Sr phase diagram section at 500ºC with 9 wt.% Al and 0.22 wt.% Mn constant. The phase Al_8Mn_5 is in small amounts stable in all phase fields. The phase $Al_{11}Mn_4$ is neglected by setting it metastable for the calculation. The field inside the thick line indicates the phase's fields containing the liquid phase L.

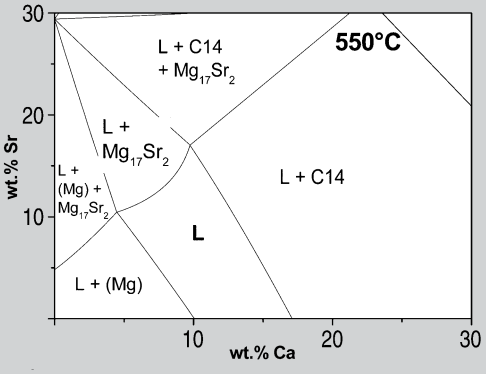

Figure 10. An Mg-Al-Mn-Ca-Sr phase diagram section at 550ºC with 9 wt.% Al and 0.22 wt.% Mn constant. The phase Al_8Mn_5 is stable in small amounts in all phase fields.

the two-phase field L + (Mg) also originates at the base alloy, which is above the solidus. In fact, all the phase fields inside the zero-phase-fraction-line of liquid, marked bold in Figure 9, demonstrate the occurrence of liquid phase together with other phases. Again, all phase fields contain small amounts of the Al_8Mn_5 phase. In addition, the less important transformation of Al_8Mn_5 to the $Al_{11}Mn_4$ phase is neglected by setting it metastable for the calculation.

Compared to Figure 6 with 3 wt.% aluminum, the Al_4Sr phase replaces $Mg_{17}Sr_2$ as the first strontium-bearing intermetallics in the 9 wt.% aluminum alloys. At the higher temperature of 550ºC, in Figure 10, the liquid phase is present in the entire phase diagram section, and even a range of totally molten alloys (except the small Al_8Mn_5 particles) is present. The $Mg_{17}Sr_2$ and C14 intermetallics are stable at rather high compositions of calcium and strontium, up to 30 wt.% in Figure 10.

MULTICOMPONENT Mg(-Al-Mn)-Ca-Sn ALLOYS

Isothermal sections of the Mg-Al-Mn-Ca-Sn system appear less complex compared to the strontium systems. Figure 11 shows an isothermal section of the Mg-Al-Mn-Ca-Sn system at 500ºC with constant 3 wt.% aluminum and 0.22 wt.% manganese. Again the phase Al_8Mn_5 is in small amounts stable in all phase fields. The CMS phase is the dominating intermetallic phase and present in almost the entire range of these alloys, except for almost vanishing tin content. For higher calcium content, C36 and C14 appear. The latter is based on Mg_2Ca with some aluminum dissolved. The Mg_2Sn phase becomes stable only above 8 wt.% tin, not shown in the cutout of Figure 11.

At 550ºC in Figure 12 an interesting "nose" of completely solid phase region (Mg)+Ca_2Sn survives up to relatively high calcium and tin content, surrounded by the partially molten region L+(Mg)+Ca_2Sn. Liquid is also stable in the other phase fields together with (Mg) or Ca_2Sn and, above 18 wt.% calcium, with C14.

The series with 9 wt.% aluminum starts again in the L + (Mg) phase field in Figure 13, as explained before with the binary diagram in Figure 8. The Ca_2Sn phase is again a dominating intermetallic, binding most of the tin in these alloys and existing in virtually all the phase fields. The same composition range at 550ºC (Figure 14) is essentially composed of L+(Mg)+Ca_2Sn, whereas C14 and C36 occur only at much higher calcium and tin content. Compared to the same section at 3 wt.% aluminum in Figure 12, the C36 occurs only in the alloys with more aluminum.

SOLIDIFICATION SIMULATION

Phase diagram calculation using a consistent multi-component database is suggested as a helpful tool for selection of promising alloy compositions. Ranges for the primary (Mg) matrix phase and for precipitation of secondary phases can easily be given. The phase diagram sections may be calculated in an entirely consistent manner for magnesium alloy composition ranges other than those exemplified here.

The usefulness of these phase diagrams is further enhanced by the fact that, using the same thermodynamic database, the solidification of individual alloys may be simulated under both equilibrium and Scheil conditions. Non-equilibrium phases may be formed at high cooling rates during casting, mainly because of the strong segregation tendency of aluminum. Thus, solidification of magnesium alloys with relevant compositions may proceed down to the lowest magnesium-rich eutectic, which is related to the ternary liquidus surfaces (see Figures 1 to 5). This solidification path due to the strong tendency of segregation can be simulated in the extreme case of blocked solid-state diffusion by using a Scheil model calculation. Figure 15 gives an example for a commercial alloy MRI135 with 8.0 wt.% Al, 1.01 wt.% Ca, 0.24 wt.% Sr, and 0.22 wt.% Mn. A logarithmic scale is selected to resolve the minority phase amounts. Five phases, γ-$Mg_{17}Al_{12}$, C15, τ, C36, Al_8Mn_5, and Al_4Sr, precipitate together with the

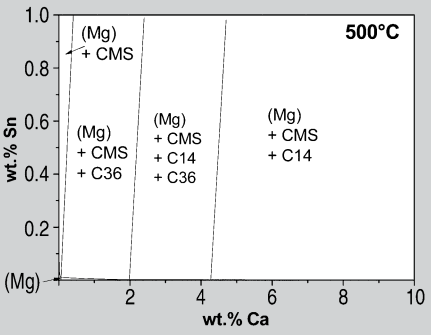

Figure 11. An Mg-Al-Mn-Ca-Sn phase diagram section at 500ºC with 3 wt.% Al and 0.22 wt.% Mn constant. The phase Al_8Mn_5 is stable in small amounts in all phase fields.

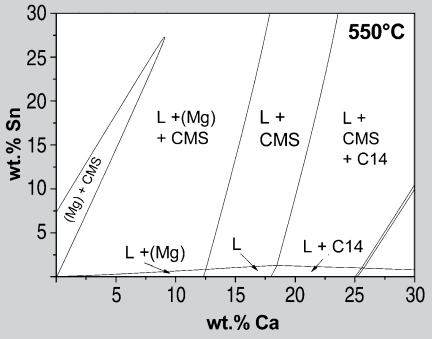

Figure 12. An Mg-Al-Mn-Ca-Sn phase diagram section at 550ºC with 3 wt.% Al and 0.22 wt.% Mn constant. The phase Al_8Mn_5 is stable in small amounts in all phase fields.

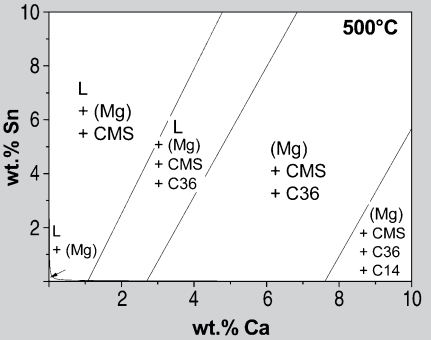

Figure 13. An Mg-Al-Mn-Ca-Sn phase diagram section at 500ºC with 9 wt.% Al and 0.22 wt.% Mn constant. The phase Al_8Mn_5 is in small amounts stable in all phase fields. The phase $Al_{11}Mn_4$ is neglected by setting it metastable for the calculation.

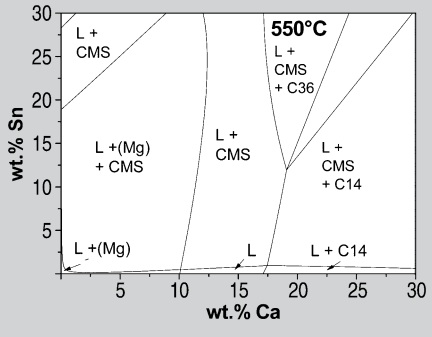

Figure 14. An Mg-Al-Mn-Ca-Sn phase diagram section at 550ºC with 9 wt.% Al and 0.22 wt.% Mn constant. The phase Al_8Mn_5 is stable in small amounts in all phase fields.

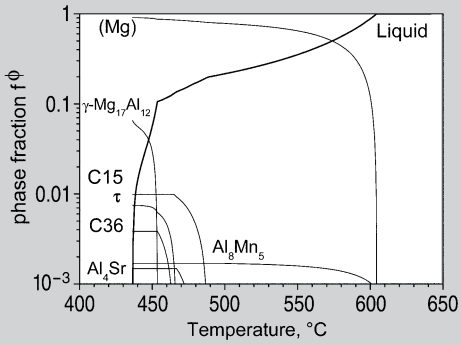

Figure 15. Simulated phase amounts during solidification under Scheil conditions for alloy MRI135 with 8.0 wt.% Al, 1.01 wt.% Ca, 0.24 wt.% Sr and 0.22 wt.% Mn, balance Mg.

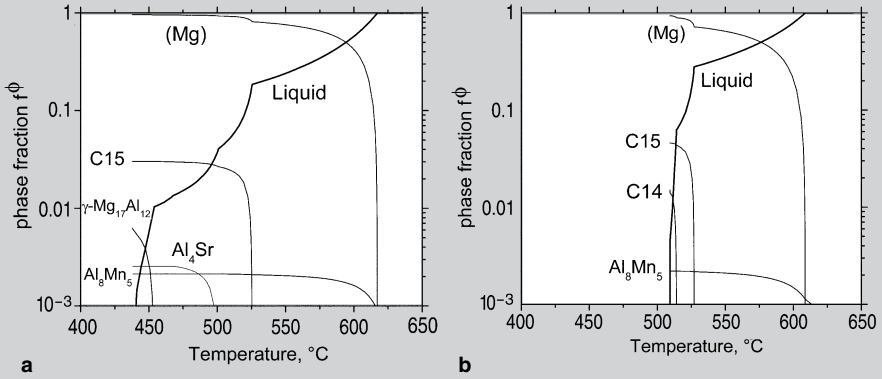

Figure 16. Simulated solidification under Scheil conditions for alloy AXJ530 with 4.8 wt.% Al, 0.2 wt.% Sr, and 0.3 wt.% Mn, balance Mg, and two different Ca contents: (a) 1.7 wt.% Ca, (b) 3.3 wt.% Ca. Additional small amounts of the following phases occur: Al11Mn4 and τ-AlMgSr in the low-Ca alloy; $Mg_{17}Sr_2$ in the high-Ca alloy. These are not shown in the diagrams because their phase fraction is below the cut-off limit of 0.001.

(Mg) matrix. By contrast, under equilibrium conditions only three phases (Al_8Mn_5, C15, and Al_4Sr), precipitate. Such quantitative results should be combined with empirical knowledge about detrimental or beneficial types of phases.

Another very important application is detecting the impact of composition variation within a given technical specification of an alloy. Which are the components that require a narrow specification because of their strong impact on phase formation and freezing range? As an example, solidification under Scheil conditions was calculated for alloy AXJ530 with a base composition Mg-4.8Al-0.2Sr-0.3Mn-xCa (wt.%) and calcium contents at the low end (1.7 wt.% calcium) and at the high end (3.3 wt.% calcium) of a technical specification. The resulting phase fractions are compared in Figure 16a and b. The dramatic impact on the freezing range is noted, 71ºC wider in the low-calcium alloy. Furthermore, in addition to (Mg), Al_8Mn_5, and Al_2Ca, significantly different phases are expected in the microstructure: γ-$Mg_{17}Al_{12}$, Al_4Sr and tiny fractions of $Al_{11}Mn_4$ and τ-AlMgSr in the low- calcium alloy only. On the other hand, Mg_2Ca and a little $Mg_{17}Sr_2$ are expected in the high-calcium alloy but not at the low end. This kind of analysis may be very useful for specifying a more proper, but not too narrow and thus costly, tolerable composition specification for all the alloying components.

ACKNOWLEDGEMENT

This study is supported by the German Research Foundation (DFG) in the Priority Programme "DFG-SPP 1168: InnoMagTec."

References

1. H.L. Lukas, S.G. Fries, and B. Sundman, *Computational Thermodynamics: The Calphad Method* (Cambridge, U.K.: Cambridge University Press, 2007).
2. R. Schmid-Fetzer and J. Gröbner, *Adv. Eng. Mat.,* 3 (2001), pp. 947–961.
3. R. Schmid-Fetzer et al., *Magnesium Technology 2007,* ed. R. Beals, M. Pekguleryuz, and N. Neelameggham (Warrendale, PA: TMS, 2007), pp. 339–344.
4. R. Schmid-Fetzer et al., *Adv. Eng. Mat.*, 7 (2005), pp. 1142–1149.
5. B.L. Mordike and T. Ebert, *Mater. Sci. Eng.*, A 302 (2001), pp. 37–45.
6. H. Dieringa et al., *Magnesium Technology 2007,* ed. R. Beals, M. Pekguleryuz, and N. Neelameggham (Warrendale, PA: TMS, 2007), pp. 3–8.
7. K.U. Kainer, editor, *Magnesium: Proc. 7th Internat. Conference on Magnesium Alloys and their Applications* (Weinheim, Germany: Wiley-VCH Verlag, 2007).
8. A.A. Luo, *International Materials Reviews,* 49 (2004), pp. 13–30.
9. M.O. Pekguleryuz and E. Baril, *Mat. Trans.,* 42 (7) (2001), pp. 1258–1267.
10. E. Baril, P. Labelle, and M.O. Pekguleryuz, *JOM,* 55 (11) (2003), pp. 34–39.
11. E.F. Emley, *Principles of Magnesium Technology* (Oxford: Pergamon Press, 1966).
12. H. Liu et al., *Mat. Sci. Eng. A,* 464 (1-2) (2007), pp. 124–128.
13. M. Ohno, D. Mirkovic, and R. Schmid-Fetzer, *Acta Mater.,* 54 (2006), pp. 3883–3891.
14. A. Prince, *MSIT Workplace*, ed. G. Effenberg (Stuttgart, Germany: MSI, Materials Science International Services GmbH, 1992), Document ID: 10.19950.1.20.
15. A. Prince, *MSIT Workplace*, ed. G. Effenberg (Stuttgart, Germany: MSI, Materials Science International Services GmbH, 1992), Document ID: 10.21613.1.20.
16. A. Prince, *MSIT Workplace*, ed. G. Effenberg (Stuttgart, Germany: MSI, Materials Science International Services GmbH, 1990), Document ID: 10.14589.1.20.
17. A. Prince, *MSIT Workplace*, ed. G. Effenberg (Stuttgart, Germany: MSI, Materials Science International Services GmbH, 1990), Document ID: 10.33760.1.20.
18. Q. Ran, *MSIT Workplace*, ed. G. Effenberg (Stuttgart, Germany: MSI, Materials Science International Services GmbH, 1992), Document ID: 10.28826.1.20.
19. A. Janz, "Thermodynamics and Constitution of Quaternary Mg-Al-Ca-Sr Alloys and the Extension to the Quinary Mg-Al-Ca-Sr-Mn System" (Ph.D. thesis, Clausthal University of Technology, Germany, 28 March 2008).
20. S.-L. Chen et al., *Calphad,* 26 (2002), pp. 175–188.
21. M. Ohno and R. Schmid-Fetzer, *Z. Metallkunde*, 96 (2005), pp. 857–869.
22. Yong Du et al., *Int. J. Materials Research (Z. Metallkunde),* 98 (2007), pp. 855–871.
23. A. Janz et al., "Thermodynamic Modeling of the Mg-Al-Ca System," *Acta Materialia* (2008) submitted.
24. A. Janz et al., *Intermetallics*, 15 (2007), pp. 506–519.
25. E. Doernberg, A. Kozlov, and R. Schmid-Fetzer, *J. Phase Equilibria & Diffusion,* 28 (2007), pp. 523–535.
26. M. Ohno et al., *Acta Mater.*, 54 (2006), pp. 4939–4951.
27. A. Kozlov et al., *Intermetallics*, 16 (2008), pp. 299–315.
28. A. Kozlov et al., *Intermetallics*, 16 (2008), pp. 316–321.

Joachim Gröbner, Andres Janz, Artem Kozlov, Djordje Mirković and Rainer Schmid-Fetzer are with the Institute of Metallurgy at Clausthal University of Technology, Robert-Koch-Str. 42, Clausthal-Zellerfeld, D-38678, Germany. Dr. Schmid-Fetzer can be reached at +49-5323-72-2150; e-mail schmid-fetzer@tu-clausthal.de.